N87-20270

MODELING TURBULENT, REACTING FLOW

Russell W. Claus
NASA Lewis Research Center
Cleveland, Ohio

This paper examines several of the approximations or models involved in the development of a numerical combustor flow code. In the first section, the importance of numerical accuracy is illustrated, and the impact that improved-accuracy schemes have on slowing convergence is demonstrated. Solution algorithms that can speed convergence are discussed and some performance features of these algorithms are illustrated. A sample calculation displaying the importance of boundary conditions on a three-dimensional numerical prediction is presented. The inaccuracy of a current turbulence model in highly turbulent (nonequilibrium) regions is described. Finally, the surprisingly good performance of a six-flux model in describing radiation heat transfer is displayed. In all the areas examined, continued research is still needed, but valuable engineering tools are available today.

INTRODUCTION

Three-dimensional combustor calculations involve detailed modeling of several important physical processes. Airflow, chemical reactions, fuel sprays, and turbulence are just a few of the physical processes that must be described. Many of these processes occur on both a molecular and a macroscopic scale. To exactly describe these processes numerically, one must resolve these scales on a computational mesh. And this is clearly beyond current computational resources. To make the computational task tractable, we introduced modeling assumptions. These modeling assumptions limit the generality of the computational flow code, but it is hoped that the dominant physics remain correctly represented.

Modeling assumptions are only the first limit of generality introduced when developing a combustor flow code. A further limit is introduced by the need to approximate the modeled equations before they are solved numerically. This approximation process can significantly affect the accuracy of a model prediction.

In view of all these factors, a combustor designer cannot be expected to fully embrace a computer model prediction. If a clear distinction between modeling errors and errors introduced by the numerical solution algorithm cannot be made, then the designer is left with a very unreliable computational tool.

This paper examines some of the compromises made when developing combustor flow codes and how these compromises affect the accuracy of turbulent flow calculations. To assess the balance of the modeling compromises, we compare a number of sample calculations with experimental data. This paper examines the five areas of numerical accuracy, solution algorithms, inlet boundary conditions, turbulence models, and radiative heat transfer.

The NUMERICAL ACCURACY section focuses on the development of more accurate numerical methods to be used in combustor flow codes. Upwind differencing, which is currently used in these flow codes, introduces an appreciable error (or numerical diffusion) into the calculation. This error may be of such a large magnitude that it obscures the turbulence model used in the calculation. A series of calculations are illustrated which demonstrate the accuracy of a variety of differencing schemes.

An important aspect of improved accuracy is the effect that the differencing scheme has on the rate of convergence. The improved accuracy schemes all appear to require more CPU time to converge. For this reason, the next section discusses solution algorithms. SIMPLE (semi-implicit pressure-linked equations) is one of the most widely used solution algorithms for solving the steady-state form of the Navier-Stokes equations. Although this scheme has proven to be quite effective, its convergence rate can be improved. This paper focuses on two approaches which accelerate convergence by performing corrections that improve the iterative agreement with continuity. These alternate schemes are illustrated in a series of calculations.

A third section examines the importance of inlet boundary conditions. An illustrative example is displayed.

The fourth section discusses turbulence models and reaction closures. Here the more pragmatic approaches to calculating turbulent reactions are illustrated. An eddy-breakup model and a PDF (probability density function) method are described and compared.

Finally, the fifth section examines the accuracy of a radiation heat-transfer model. A six-flux model of radiative heat transfer is described. This model provides only a limited geometric description of the radiation transfer process, but a comparison with experimental data indicates an encouraging level of agreement.

NUMERICAL ACCURACY

The following is a general form of the time-averaged equations that must be solved in a combustor flow code:

$$\frac{\partial}{\partial x}(\rho U\varphi) + \frac{\partial}{\partial y}(\rho V\varphi) - \frac{\partial}{\partial x}\left(\Gamma_\varphi \frac{\partial \varphi}{\partial x}\right) - \frac{\partial}{\partial y}\left(\Gamma_\varphi \frac{\partial \varphi}{\partial y}\right) = S_\varphi \qquad (1)$$

where φ can represent U, V, W, $\overline{u_i u_j}$, K, ϵ, or H; where Γ_φ is the diffusion coefficients (e.g., μ_{eff}); and S_φ is the source term (e.g., $-\partial P/\partial x$). The equation represents convection of a conserved scalar that is subtracted by diffusion terms equal to a source term that could represent a pressure gradient or a source/sink term. These equations are solved by discretizing on a staggered mesh using the finite volume method (fig. 1). The staggered mesh system is used to avoid the pressure-velocity decoupling that can result in a finite volume representation of incompressible flow.

An example of the discretization of a convective term using central differencing is the following:

$$\frac{1}{\Delta x \Delta y} \iint \frac{\partial \rho u \varphi}{\partial x} \, dx \, dy \approx \frac{(\rho u \varphi)_e - (\rho u \varphi)_w}{\Delta x} \tag{2}$$

(Alternate types of differencing are possible and some will be illustrated in the following paragraphs.) Once all the terms have been approximated, like terms are then rearranged in a substitution formula which can be solved using a tri-diagonal matrix algorithm (TDMA) procedure applied in alternate directions (ADI):

$$\alpha_P \varphi_P = \alpha_N \varphi_N + \alpha_S \varphi_S + \alpha_E \varphi_E + \alpha_W \varphi_W + S \tag{3}$$

where, for example,

$$\alpha_N = \left[\frac{\Gamma_n}{\delta_y} - \frac{(\rho V)_n}{2} \right] \Big/ \Delta y_j$$

The source and diffusive terms in these equations are approximated using central differencing which is second-order accurate (Error $\propto O(\Delta x)^2$). The convective terms have typically been differenced using hybrid differencing which reverts to upwind differencing when the absolute value of the cell Reynolds number, or cell Peclet number, is greater than 2, which is the main reason for the loss of numerical accuracy. An example of convective discretization using hybrid differencing is as follows:

$$\frac{\partial u \varphi}{\partial x} \approx \frac{(u \varphi)_e - (u \varphi)_w}{\Delta x} \tag{4}$$

For upwind, with $u > 0$,

$$(u \varphi)_e = u_e \varphi_p$$

and

$$(u \varphi)_w = \frac{1}{2} u_w (\varphi_w + \varphi_p)$$

Since upwind differencing is only first-order accurate, it can introduce an extensive amount of numerical diffusion into the calculation. The virtue of this scheme is that it provides "bounded," stable solutions. Higher order convective schemes invariably yield nonphysical oscillations in the solution. Upwind differencing avoids this, at a considerable loss in accuracy.

To alleviate this problem, NASA has conducted a program to identify and incorporate an improved accuracy differencing scheme into a combustor flow code. Under a portion of this program a variety of differencing schemes were examined in several test calculations. The schemes examined included QUICK (quadratic upstream interpolation) and SUD (skewed upwind differencing). QUICK differencing was developed by Leonard (ref. 1). This scheme improves the accuracy of convective differencing by performing an upwind biased quadratic interpolation. For $u > 0$,

$$\left.\begin{aligned}(u\varphi)_e &= u_e\left(-\frac{1}{8}\varphi_W + \frac{3}{4}\varphi_P + \frac{3}{8}\varphi_E\right)\\ (u\varphi)_w &= u_w\left(-\frac{1}{8}\varphi_{WW} + \frac{3}{4}\varphi_W + \frac{3}{8}\varphi_P\right)\end{aligned}\right\} \qquad (5)$$

where grid point locations are as noted on figure 2. This scheme is second-order accurate and can produce nonphysical oscillations in the solution. SUD (skewed upwind differencing) (ref. 2) attains high accuracy by differencing in an upwind manner along the flow streamlines. While maintaining the same formal accuracy as upwind differencing, the truncation error in SUD is smaller. For example:

For $u > 0$ and $V > 0$,

$$\left.\begin{aligned}(u\varphi)_e &= u_e\varphi_P\\ (u\varphi)_w &= u_w(1-\alpha)\varphi_W + u_w\alpha\varphi_{SW}\\ V &= \text{minimum of } (1, V/2u)\end{aligned}\right\} \qquad (6)$$

where grid point locations are as noted in figure 3. As with QUICK, SUD can produce nonphysical oscillations in the solution; therefore, a scheme to "bound" SUD was also examined. This scheme employs the concept of flux-blending (ref. 3), wherein a bounded flux determined from upwind differencing is blended with the unbounded, but more accurate, SUD flux. The main factor is to blend as little of the lesser accurate scheme while still maintaining a properly "bounded" solution. This procedure, called BSUDS, starts from an initial, totally skew-differenced estimate and blends an upwind flux if the solution is out of the range of neighboring values. If the solution is in range (i.e., bounded), then no blending is performed.

An illustration of the accuracy of the upwind, QUICK, and SUD schemes is seen in figure 4. This figure displays the results of a single-point scalar-transport calculation made for various flow angles. All schemes agree with an exact solution (no error) at a zero flow angle; however, at angles greater than zero, each scheme displays some degree of error relating to numerical diffusion. The error displayed by upwind differencing increases with flow angle to a maximum at 45°. The QUICK scheme displays a similar behavior, but the overall error is much less. The SUD scheme displays a maximum error around 15°, but it tends to zero at angles approaching 45°. Both QUICK and SUD display a much higher level of accuracy than upwind.

Although a scalar transport calculation is useful for a general examination of some aspects of differencing scheme performance, a laminar flow calculation is a more complete test. The results of a series of laminar flow calculations from reference 4 are displayed in figure 5. In this figure, axial velocity profiles at a distance of one-half a duct height from the inlet are shown for two different computational meshes. In these calculations, the steepness of the velocity profile indicates accuracy. Steep velocity profiles are exhibited by QUICK and BSUDS; the upwind profiles exhibit a high degree of numerical diffusion. On the coarse mesh, BSUDS appears to be more accurate than QUICK; on the fine mesh, there is not much of a distinction between the two schemes.

An important aspect of improved accuracy is the effect that the differencing scheme has on the rate of convergence. The computational times to converge the system of governing equations in the previous laminar calculations are shown in table I. The convergence times are ratioed to the upwind convergence times to clearly illustrate the computational penalty paid to attain improved accuracy. Generally, the improved accuracy schemes required from 3 to 15 times longer to reach a converged solution. To a degree one can hope that this computational penalty can be offset by using coarse meshes to achieve the same overall level of accuracy. In reality, a relatively fine mesh is needed, even with the high-accuracy schemes. In any case, the need for improved solution algorithms for these more accurate differencing schemes is strongly indicated.

SOLUTION ALGORITHMS

The previous section demonstrated the need for improved solution algorithms. This section examines the widely used SIMPLE algorithm and two modifications to this scheme. These schemes cover only a small portion of the wide range of methods to accelerate solution convergence. Vectorization, direct-solution methods, and multigrid methods - to list just a few - are all areas of active research that are certain to yield much greater computational benefits in the near future.

In the SIMPLE algorithm, a guessed pressure field is inserted into the discretized momentum equations to obtain a velocity field. The pressure field is corrected by an equation which is derived through a combination of the continuity and momentum equations. The velocity field is then updated and is used in the solution of the equations for k, ε, and φ. The corrected pressure field is treated as the guessed pressure field, and the procedure is repeated until a converged solution is obtained.

The following velocity correction equation is used in the SIMPLE scheme for u at point e:

$$A_e u'_e = \sum_{nb} \underline{A_{nb} U'_{nb}} + (P'_P - P'_E)A_e \qquad (7)$$

Primes indicate corrections to old values. The underlined term, which represents the influence of corrected pressures on neighboring velocities, is neglected in the SIMPLE algorithm. The converged solution is unchanged by the exclusion of this term since, for the steady-state solution, the corrections go to zero. Neglecting terms, however, does force the use of low underrelaxation factors, which can slow convergence.

The SIMPLER algorithm improves on the SIMPLE scheme by including the previously neglected terms when calculating the pressure field. The calculation sequence starts with a guessed velocity field. An equation that solves for the pressure field (using the terms ignored in the SIMPLE scheme) is calculated from the guessed velocity field. This pressure field is then used to solve the discretized momentum equations to obtain a velocity field. The velocity field is corrected in a manner similar to the SIMPLE velocity correction. This velocity field is then treated as the guessed velocity field, and the iteration procedure is repeated until convergence is reached.

Because additional equations are solved, each iteration through the SIMPLER routine involves more computational time than an iteration step through SIMPLE. However, higher underrelaxation factors can be applied in the SIMPLER routine, thereby accelerating convergence.

The PISO scheme also takes into account the terms neglected in the SIMPLE code, but in a different manner. The PISO routine mimics the SIMPLE approach until the end of the first iteration. At this point, the PISO scheme employs an equation containing the neglected terms to correct the pressure and velocity field to more closely agree with continuity. Again, this procedure is repeated until the solution converges. In this manner, the PISO code allows for higher underrelaxation factors to accelerate convergence.

The performance of these various solution schemes is displayed in figure 6. As an example, the convergence times for a 38-by-38 grid point calculation are plotted as a function of underrelaxation factor (fig. 6(a)). When a reasonably large underrelaxation factor is used, SIMPLER or PISO converge about twice as fast as SIMPLE. In addition, SIMPLER and PISO converge over a larger range of underrelaxation factors than SIMPLE. From an engineering standpoint, improving the "robustness" of a computational scheme is often just as important as accelerating convergence. The computational benefit of using SIMPLER and PISO for fine-mesh calculations is displayed in figure 6(b). The greater the number of mesh points used in the calculation, the greater the benefit of SIMPLER or PISO over SIMPLE. For example, a calculation of approximately 3300 grid points converges three times faster using PISO or SIMPLER than it does using SIMPLE. This is a savings of about 600 CPU seconds. The 1440 grid points calculation demonstrated a savings of only about 100 CPU seconds.

INLET BOUNDARY CONDITIONS

In any calculation of a complex, three-dimensional turbulent flow, the boundary conditions that are needed in the calculation are frequently unknown or unmeasured. The use of inappropriate values at the computational boundary can sometimes be the main limit to the calculation's predictive capability. This error can sometimes be more important than numerical accuracy or turbulence model considerations. Figure 7 shows an example of a three-dimensional jet-in-crossflow calculation using alternate boundary conditions. In one calculation, the jet orifice flow was specified as having a uniform plug flow at a position two jet diameters upstream of the orifice outlet. This allowed the flow to distort as it exited the orifice outlet. The second calculation specified a uniform plug flow at the orifice outlet. The resulting axial velocity profiles are compared with experimental data in figure 8. Somewhat surprisingly, the uniform boundary condition at the orifice compared more favorably with experimental data than the theoretically more correct distorted profile. This should not be interpreted as an endorsement of the use of uniform-plug-flow boundary conditions for these types of flows. Indeed, there is some indication of experimental error (ref. 5). This example is meant only to illustrate that unmeasured or unknown boundary conditions can significantly affect a numerical calculation.

TURBULENCE MODELS

Although a great deal of progress is being made in solving the three-dimensional, time-dependent Navier-Stokes equations in large-eddy or direct

numerical simulations, practical engineering calculations currently require the introduction of some form of turbulence modeling. These models are based on either Reynolds or Favre averaging of the exact Navier-Stokes equations, reducing the unsteady form of these equations to an averaged form. Currently, the most widely used turbulence model is the two equation, k-ε, closure. This model relates the Reynolds stresses to a turbulent viscosity through Boussinesq's eddy-viscosity concept:

$$-\rho\overline{u_i u_j} = \rho\nu_T\left(\frac{\partial U_i}{\partial x_j} + \frac{\partial U_j}{\partial x_i}\right) - \frac{2}{3}\,\delta_{ij}k \tag{8}$$

where $\nu_T = C_\mu k^2/\varepsilon$. The turbulent viscosity is related to the kinetic energy k and the dissipation rate ε of the turbulence. The transport equations are then solved for k and ε:

$$\left.\begin{aligned} U_i\,\frac{\partial k}{\partial x_i} &= \frac{\partial}{\partial x_i}\left(\frac{\nu_T}{\sigma_k}\,\frac{\partial k}{\partial x_i}\right) + \nu_T\left(\frac{\partial U_i}{\partial x_j} + \frac{\partial U_j}{\partial x_i}\right)\frac{\partial U_i}{\partial x_j} - \varepsilon \\ U_i\,\frac{\partial \varepsilon}{\partial x_i} &= \frac{\partial}{\partial x_i}\left(\frac{\nu_T}{\sigma_\varepsilon}\,\frac{\partial \varepsilon}{\partial x_i}\right) + C_{\varepsilon 1}\,\frac{\varepsilon}{k}\,\nu_T\left(\frac{\partial U_i}{\partial x_j} + \frac{\partial U_j}{\partial x_i}\right)\frac{\partial U_i}{\partial x_j} - C_{\varepsilon 2}\,\frac{\varepsilon^2}{k} \end{aligned}\right\} \tag{9}$$

Where $C_\mu = 0.09$, $C_{\varepsilon 1} = 1.44$, $C_{\varepsilon 2} = 1.92$, $\sigma_k = 1.0$, $\sigma_\varepsilon = 1.3$, $\sigma_\varphi = 0.9$, $k = (1/2)(\overline{u'^2} + \overline{v'^2} + \overline{w'^2})$ and $\varepsilon = C_\mu k^{3/2}/\ell_T$.

The model constants typically employed are those recommended in reference 6. The turbulent Schmidt number σ_φ, is frequently changed from 0.9 to as low as 0.2, depending on the flow being studied.

This two-equation model is based on several assumptions which should be considered when making a numerical calculation. First, the flow is assumed to be close to equilibrium; that is, the flow properties change relatively slowly. Second, the turbulence Reynolds number is assumed to be high. Third, the turbulence is assumed to be isotropic.

The main concern is how well this model, with its inherent assumptions, can represent combustorlike flow fields. Figure 9 displays a comparison between laboratory experiments and numerical predictions of two different isothermal flows. (Figs. 10 and 11 show the locations of the measurements that were made in the flow fields.) In the two-dimensional bluff-body comparison, a major disagreement between measurements and predictions is evident at an axial distance x/D of approximately 0.8. This corresponds to the end of the recirculation zone and causes an incorrect prediction of recirculation zone length. The jet-in-crossflow comparison displays a similar disagreement in the region where the turbulence intensity is high. In this comparison, both hybrid and BSUDS differencing were used in the predictions. It is obvious from the displayed results that numerical accuracy can have a major impact on the comparison with experimental measurements. Hybrid differencing is so completely influenced by numerical diffusion that the qualitative agreement between experiment and calculation, evident in the BSUDS results, is eliminated. The BSUDS results are not grid-independent, but it seems unlikely that this will fully explain the noted disparity.

Both of these flow fields display the greatest disagreement between experiment and calculation where the turbulence intensities are the highest. These are regions where the flow field is likely to be far from equilibrium. It is interesting to note that a full Reynolds stress transport (RST) model calculation (presented by McGuirk, J.J., Papadimitriou, C., and Taylor, A.M.K.P. at the Fifth Symposium on Turbulent Shear Flows held at Cornell University, Ithaca, New York, August, 1985) did not yield appreciably better results for a similar flow field. Because both models appear to lose validity around the region of the stagnation point, further model development is needed.

Reaction closures involve a further series of assumptions and approximations. The simplest level of closure is to assume that the reaction is mixing limited and ignore the effect of temporal density fluctuations. The reaction rate can then be related to an eddy lifetime (ε/k) using either a Magnussen-Hjertager or Spaldings eddy-breakup model:

$$\text{Rate} = -S_{m_F} \tag{10}$$

where

$$S_{m_F} = -\rho \frac{\varepsilon}{k} \min\left[Am_F,\ A \frac{Mo_2}{STOIC},\quad AB \frac{M_{\rho r}}{STOIC + 1}\right]$$

or

$$S_{m_F} = -C_R \rho \frac{\varepsilon}{k} m_{Fu}^2$$

where A, B, and C_R are empirical constants and ε/k can be considered as the eddy lifetime. The density and temperature throughout the flow field can then be established from equilibrium chemistry.

Improved physical realism can be added to this model by introducing the probability density function (PDF) for mixture fraction f. This can account for the unsteady time history of the mixture fraction at each point in space. A nonlinear functional dependence between concentration, temperature, and density occurs as pockets of alternately hot and cold gases are swept past each point in space. Integrating the resultant PDFs allows a determination of the mean properties of the flow.

Figure 12 displays the results of both an eddy-breakup and a PDF model calculation of a planar-mixing layer. The PDF model calculations (ref. 7) demonstrate a significant improvement over the eddy-breakup results. The main factor involved in this improvement is the more physically correct representation of the mixture fraction variation at the point of maximum temperature rise. Of course, both of these models are only as good as the turbulence closure and are wholly inadequate when finite-rate chemistry is important.

RADIATION HEAT TRANSFER

The final topic to be covered in this review concerns radiative heat transfer. Radiation is one of the most significant and least understood heat loads to the combustor liner. It can also play a significant role in the

determination of flame temperature. Any numerical description of a gas turbine combustor must include a radiation heat-transfer model. The six-flux model is the model most commonly used to approximate multidimensional radiative transfer. In this model, differential equations describing the radiative fluxes in positive and negative directions along the principal axis are solved:

$$\left.\begin{aligned}
\frac{d}{dx}\left(\frac{1}{a+S}\frac{dR^x}{dx}\right) &= a(R^x - E) + \frac{S}{3}(2R^x - R^r - R^z) \\
\frac{1}{r}\frac{d}{dr}\left(\frac{r}{a+S+\frac{1}{r}}\frac{dR^r}{dr}\right) &= a(R^r - E) + \frac{S}{3}(2R^r - R^x - R^z) \\
\frac{1}{r}\frac{d}{d\theta}\left(\frac{1}{a+S}\frac{dR^z}{r\,d\theta}\right) &= a(R^z - E) + \frac{S}{3}(2R^z - R^x - R^r)
\end{aligned}\right\} \qquad (11)$$

where

$R^{x,r,z}$ composite fluxes

a absorption coefficient

S scattering coefficient

E σT^4

The main input to this analysis concerns the optical characteristics of the hot gas and soot which must be arbitrarily specified or calculated through a soot formation and oxidation model.

The performance of the six-flux model (ref. 8) is displayed in figure 13. Although the model overestimates the radiative heat transfer in comparison with experimental data, the qualitative trend is quite closely followed. Given the large number of approximations used in the analysis, the agreement with experimental data is quite surprising. The six-flux model does not accurately treat the angular dependence of energy transfer, and the determination of the optical characteristics of the soot cloud still remains as an area of needed research; however, fairly good results appear to be possible in this example.

CONCLUDING REMARKS

Perhaps the most important question any review on numerical modeling can answer is whether or not current computational codes can be usefully employed in the design of combustion devices. Certainly a great deal of research is needed before one can expect quantitative predictive accuracy, and it seems likely that some hardware problems will only be resolved through development testing. The best computer program will never replace the designer's innovative mind, but computer predictions can be used to extend the designer's productivity. New designs can be examined much more rapidly on the computer than in hardware testing. Development costs can be reduced. The promise of this computer-based design methodology is so great that these numerical models will be used despite their deficiencies. Designers should not and probably will

not abandon empirical design tools, but the cautious adoption of numerical models in the design process is a trend which can reap important benefits.

REFERENCES

1. Leonard, B.P.: Stable and Accurate Convective Modelling Procedure Based on Quadratic Upstream Interpolation. Comput. Methods Appl. Mech. Eng., vol. 19, no. 1, June 1979, pp. 59-98.

2. Raithby, G.D.: Skew Upstream Differencing Schemes for Problems Involving Fluid Flow. Comput. Methods Appl. Mech. Eng., vol. 9, no. 2, Oct. 1976, pp. 153-164.

3. Boris, J.P.; and Book, D.L.: Flux Corrected Transport. I. SHASTA, A Fluid Transport Algorithm That Works. J. Comput. Phys., vol. 11, no. 1, Jan. 1973, pp. 38-69.

4. Claus, R.W.; Neely, G.M.; and Syed, S.A.: Reducing Numerical Diffusion for Incompressible Flow Calculations. NASA TM-83621, 1984.

5. Claus, R.W.: Numerical Calculation of Subsonic Jets in Crossflow With Reduced Numerical Diffusion. NASA TM-87003, 1985.

6. Launder, B.E.; and Spalding, D.B.: The Numerical Computation of Turbulent Flows. Comput. Methods Appl. Mech. Eng, vol. 3, no. 2, Mar. 1974, pp. 269-289.

7. Farchshi, M.: Prediction of Heat Release Effects on a Mixing Layer. AIAA Paper 86-0058, Jan. 1986.

8. Srivatsa, S.K.: Computations of Soot and NO_x Emissions From Gas Turbine Combustors. (GARRETT-REPT-21-4309, Garrett Turbine Engine Co.; NASA Contract NAS3-22542.) NASA CR-167930, 1982.

TABLE I. - RATIO OF CONVERGENCE TIMES
FOR VARIOUS DIFFERENCING SCHEMES
WITH UPWIND CONVERGENCE TIMES
USED AS THE STANDARD

Mesh	Upwind	BSUDS	QUICK
Coarse (30 by 22)	1	6.4	3.2
Fine (58 by 38)	1	14.7	15.7

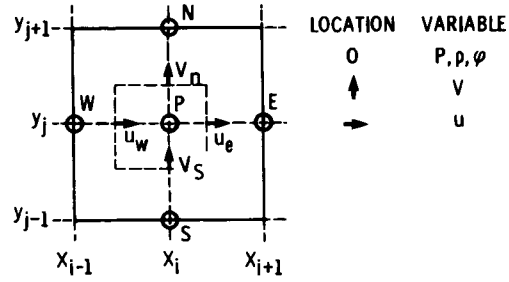

Figure 1. - Staggered mesh system for discretizing equations by finite volume method.

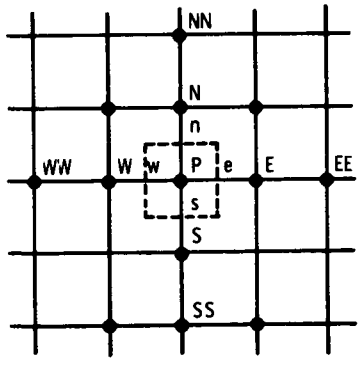

Figure 2. - Staggered mesh system for quadratic upstream interpolation.

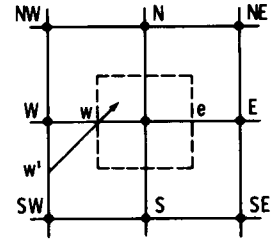

Figure 3. - Staggered mesh system for bounded skew upwind differencing scheme (BSUDS).

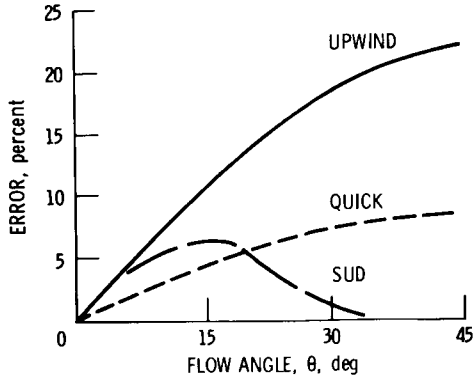

Figure 4. - Accuracy of various differencing schemes for a scalar transport test calculation.

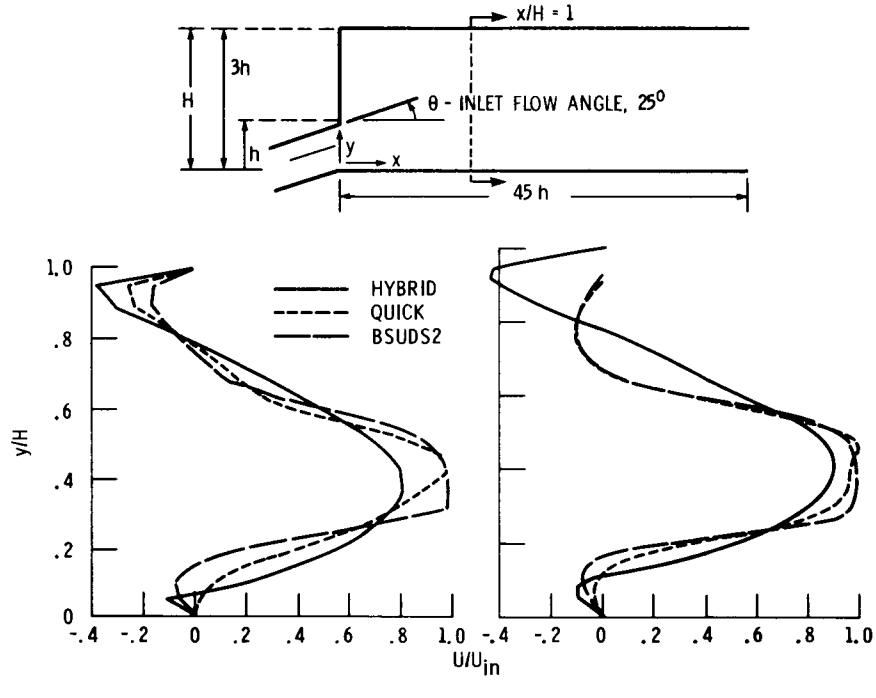

(a) Coarse grid calculations, 30 by 22. (b) Fine grid calculations, 58 by 38.

Figure 5. - Laminar flow calculations testing various differencing schemes.

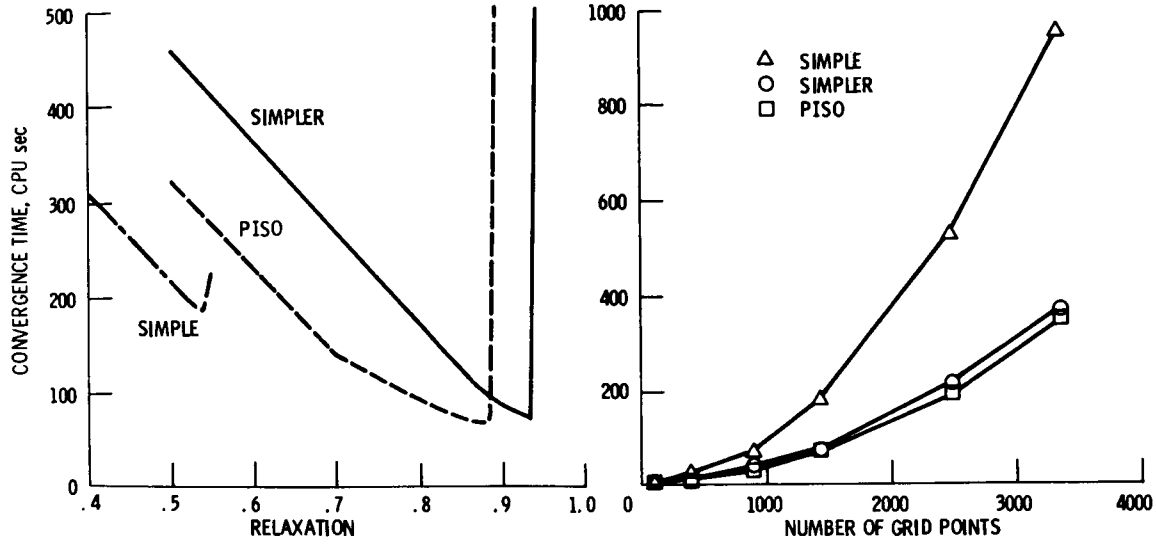

(a) For 38 by 38 grid point calculation.

(b) For various computational meshes.

Figure 6. - Convergence times.

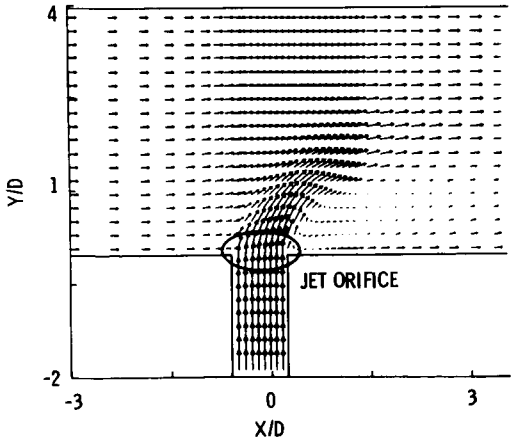

Figure 7. - Three-dimensional jet-in-crossflow calculation.

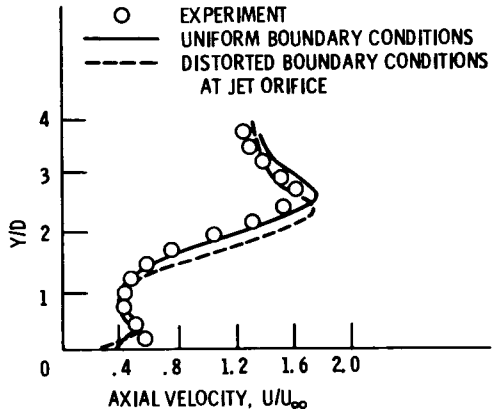

Figure 8. - Calculated axial velocity profiles compared with experimental data.

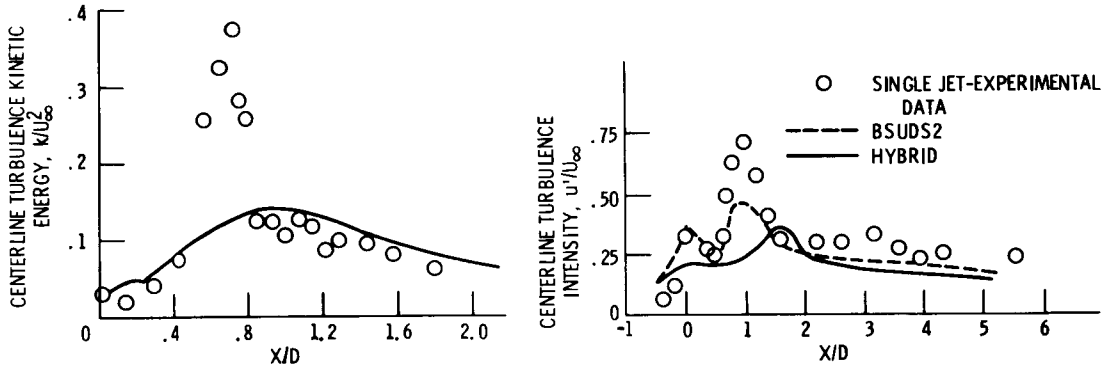

(a) Two-dimensional bluff-body wake.

(b) Three-dimensional jets in crossflow.

Figure 9. - Comparison of laboratory experiments with numerical predictions of two different isothermal flows.

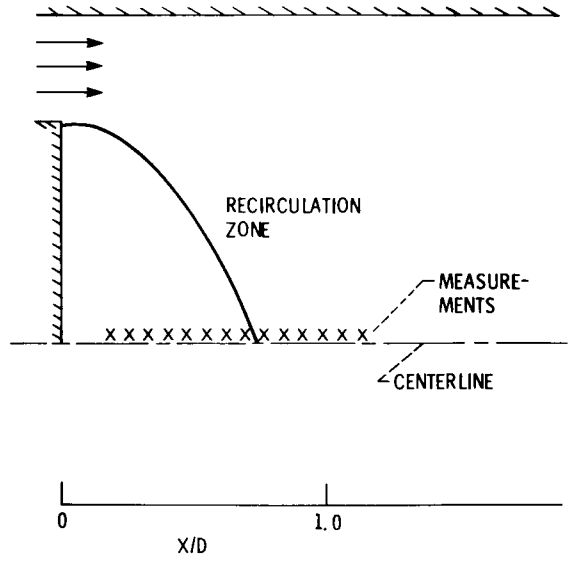

Figure 10. - Two-dimensional bluff-body geometry.

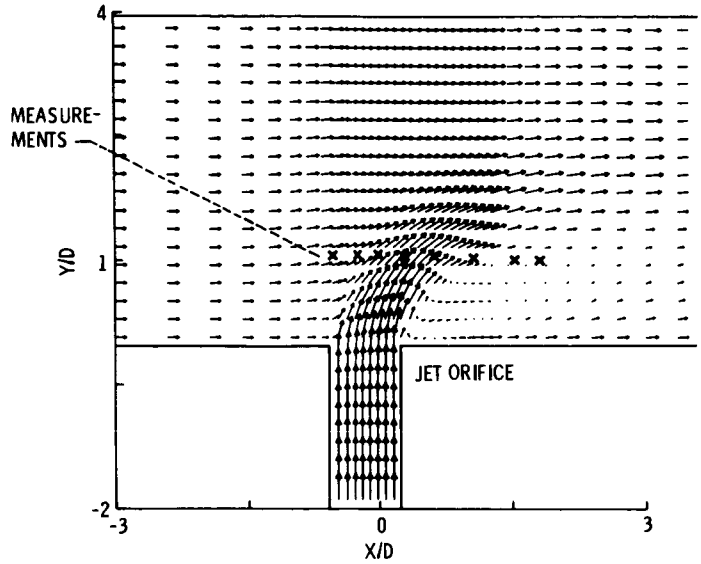

Figure 11. - Three-dimensional jet geometry.

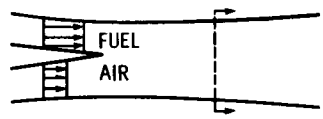

(a) Example - planar mixing layer.

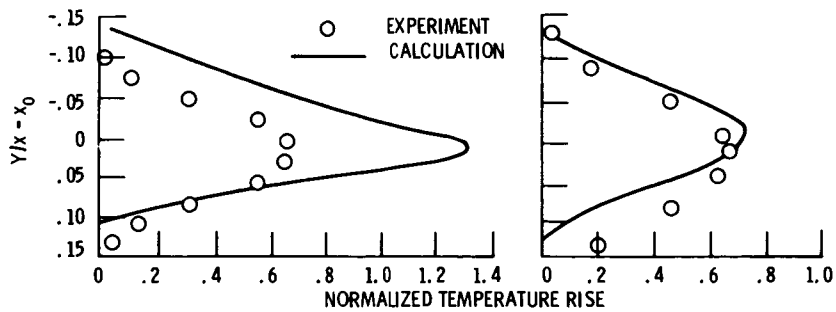

(b) Eddy breakup model. (c) PDF model.

Figure 12. - Results of calculations of a planar-mixing layer.

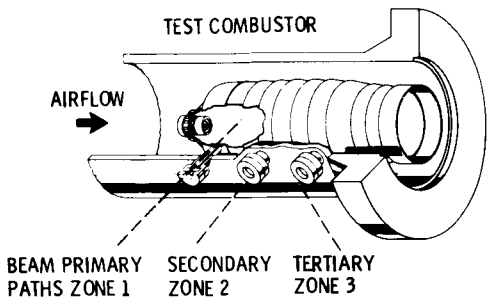

(a) Schematic drawing of experimental measurement locations.

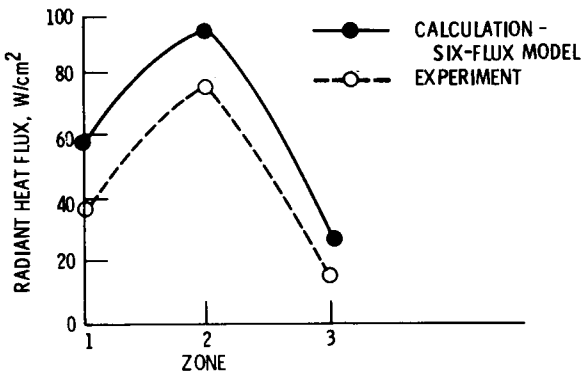

(b) Performance of six-flux model.

Figure 13. - Radiative heat transfer test calculation.